Journal of Thermal Analysis, Vol. 51 (1998) 105-114

THERMAL TRANSITIONS AND STATE OF WATER IN BINARY MIXTURES OF WATER AND *n*-DECANE-PHOSPHONIC ACID OR ITS SODIUM SALTS

J. F. A. Soltero[1], *J. E. Puig*[1] *and P. C. Schulz*[2]

[1]Departamento de Ingeniería Química, Universidad de Guadalajara
Boul. M. García Barragán # 1451, Guadalajara, Jal. 44430, México
[2]Departamento de Química y de Ingeniería Química, Universidad Nacional del Sur
Bahía Blanca 8000, Argentina

Abstract

The state of water and several transitions were examined in the systems *n*-decanephosphonic acid (DPA)–water and the sodium salts of DPA–water. Temperature – composition phase diagrams are reported. The results show that several liquid crystalline phases plus isotropic liquid, and two solid phases (a waxy solid phase and a crystalline phase) are formed. Several types of water were detected: bulk-like water, interfacial water and hydration water.

Keywords: alkanephosphonic acid, DSC thermal transitions, phase behavior

Introduction

Surfactant-based liquid crystalline phases are currently the subject of vigorous research because of their scientific and technological applications [1–4]. Weakly polar amphiphile compounds such as low molecular weight alcohols and fatty acids usually do not form liquid crystalline phases with water or other solvents. Alkanephosphonic acids have polarities similar to those of fatty acids [5], and it was therefore believed that they would not form liquid crystals in water either. However, Klose *et al.* [6] found lamellar phases in mixtures of water and *n*-alkanephosphonic acids containing seven or eight carbons. More recently, Schulz *et al.* [7] reported that the use of differential scanning calorimetry (DSC), polarized light microscopy and FTIR spectroscopy revealed the formation of several liquid crystalline phases in the systems *n*-decanephosphonic acid (DPA)-water and *n*-decanephosphonic acid–water. Besides their usual phase behavior [6, 7], alkanephosphonic acids have many applications. They are used as corrosion inhibitors [8], as metal sequestrants [9] and as collectors for recovery of metals by flotation [10].

Several types of water have been detected in surfactant-based liquid crystalline systems [11–15]. The enthalpies and temperatures of melting of the inter-

0368–4466/98/ $ 5.00

Akadémiai Kiadó, Budapest
Kluwer Academic Publishers, Dordrecht

facial and bound water are different from those of the bulk water and they exhibit unusually low supercooling temperatures [13]. The supercooling and freezing behavior of water in non-bulk states is important in comprehending how water behaves in foods, gels, biological tissues, microstructured fluids and other complex systems at sub-zero temperatures. In this paper, we examine the water behavior and other thermal transitions in binary mixtures of water and surfactants that form liquid crystalline phases. The surfactants examined were (DPA) monosodium *n*-decanephosphonate (NaHDP) and disodium *n*-decanephosphonate (Na_2DP).

Experimental section

The synthesis and purification of DPA are described elsewhere [16, 17]. Because of the large differences in the pK's of DPA (pK_1=3.98 and pK_2=7.90) [18], the monosodium and disodium salts of DPA are simply prepared by dissolving a known amount of DPA in methanol and mixing with a methanolic solution of NaOH of appropriate concentration, the methanol is then removed by vacuum drying to yield the solid salt. Water was doubly distilled and deionized.

Samples were prepared by weighing water and DPA or the salt in vials, which were hermetically sealed and maintained at 100°C for 1 h with constant agitation. Then samples were allowed to stand at room temperature for 2 days before DSC, FTIR or microscopic examination.

DSC curves were obtained with a Perkin Elmer DSC-4 differential scanning calorimeter. The instrument was calibrated with indium, water and *n*-octane standards. Cooling scans were run with the aid of an Intracooler I refrigeration unit (Perkin Elmer). All curves were obtained at heating and cooling rates of $10°C\ min^{-1}$. Aluminium pans were used for volatile samples to minimize losses by evaporation. Samples were weighed before and after DSC runs. Results on samples that lost mass were discarded.

IR spectra were taken with a Nicolet 5ZDA FTIR spectrometer equipped with a thermostated Irtran cell. A Meopta Praha polarizing microscope furnished with a photographic camera and a hot-cool stage was used to examine the textures of the sample. The stage has a thermocouple to measure the temperature of the sample.

Results

Representative DSC curves of DPA–water mixtures upon heating or cooling are shown in Fig. 1. When pure DPA is heated, three thermal transitions are detected (Fig. 1: DSC curves for 100% DPA). These transitions are labelled 1–3 in the phase diagram shown in Fig. 2. The first transition, at 44°C, has an enthalpy of $97.5\pm8.8\ J\ g^{-1}$. The second transition takes place at 53°C, with an enthalpy of $21.3\pm0.2\ J\ g^{-1}$. The last transition, occurring at 89°C, has an enthalpy of $59\pm3.8\ J\ g^{-1}$.

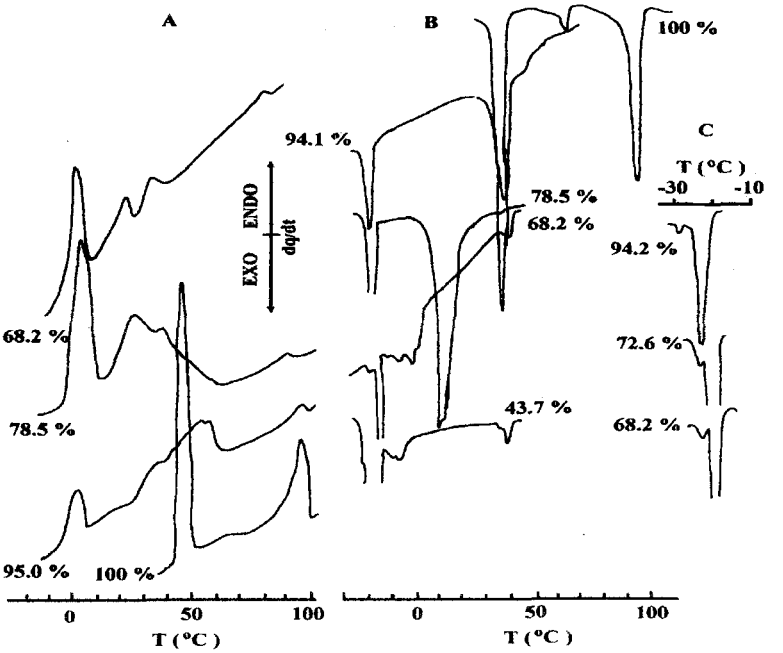

Fig. 1 Representative DSC curves of the DPA–water system: (A) by heating; (B) by cooling; (C) amplification of the water freezing peaks. Concentrations are in wt.% DPA

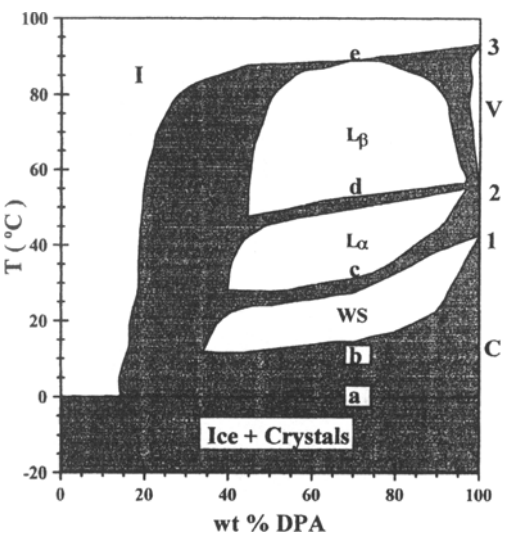

Fig. 2 Phase diagram for the DPA–water system: V: cubic phase; L_α: low-temperature lamellar phase; L_β: high-temperature lamellar phase; C: crystals; I: isotropic liquid; WS: waxy solid

Upon addition of water, all the transitions detected for pure DPA become weaker and broader because the crystalline structure of the pure amphiphile is disrupted (DSC curve for 95% DPA in Fig. 1). Two other transitions are observed with increasing water content in the sample: one at 0°C, which corresponds to the melting of water, and another at around 15°C, which shifts to higher temperatures as the DPA concentration increases. These five transitions are denoted **a–e** with increasing temperature in the phase diagram (Fig. 2). The natures of these transitions were elucidated by FTIR spectroscopy and polarized light microscopy. Details are given elsewhere [7].

All the transitions showed supercooling (Fig. 1b). In particular, in cooling runs two different peaks for the solidification of water were detected. The transition temperatures of the supercooling shifts to lower values as the water content in the sample decreases (Fig. 1c).

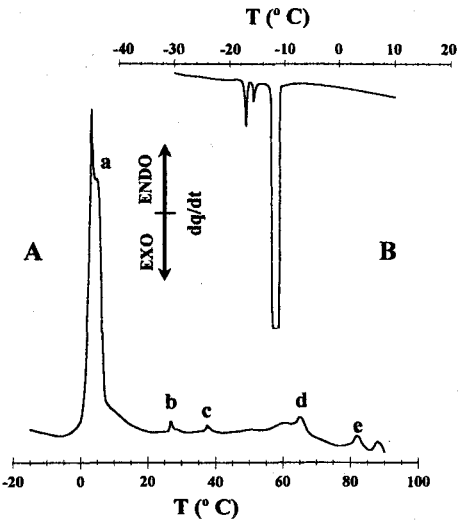

Fig. 3 Representative DSC curves of the NaHDP–water system: (A) by heating; (B) by cooling. Concentrations are in wt.% NaHDP

Representative DSC curves for the system NaHDP–water are shown in Fig. 3. With the aid of optical microscopy and FTIR spectroscopy, the temperature – composition phase diagram was obtained (Fig. 4). The composition NaHDP·$5H_2O$ was obtained by crystallization of a 6-month-old saturated solution. The water content was determined by differences in mass. Attention is drawn to the presence of two small peaks next to the transition at 0°C (which is due to the melting of ice). These peaks, at –2 and –5°C, are related to the melting of interfacial water. Similar curves have been reported for other water–surfactant liquid crystalline phases [11, 13].

The phase diagram of the system Na_2DP–water, shown in Fig. 5, was again obtained with a combination of DSC, optical microscopy and FTIR spectros-

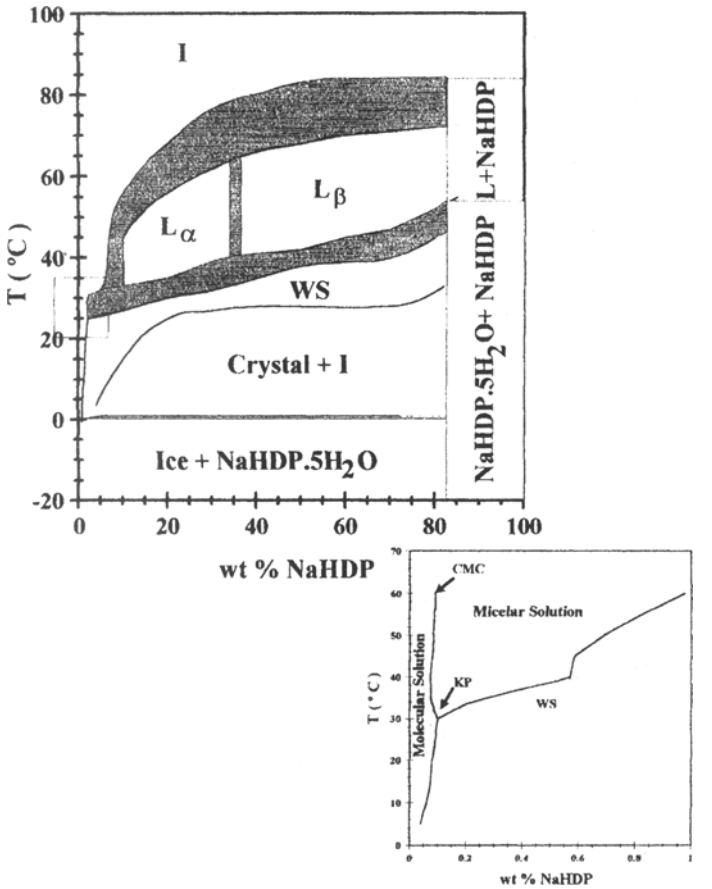

Fig. 4 Phase diagram for the NaHDP–water system: H: hexagonal phase; L: lamellar phase; C: crystals; I: isotropic liquid; WS: waxy solid

copy. The composition $Na_2DP{\cdot}4H_2O$ was determined by crystallization of a 6-month-old saturated sample. The *cmc* boundary was drawn from data taken from the literature [19]. Similarly as in the system NaHDP–water, three peaks associated with different types of water were detected (not shown).

The enthalpies of melting of water are shown in Fig. 6 for the three systems examined. When plotted per gram of water, the melting enthalpy of water for the system DPA–water, obtained by extrapolation to 100 wt.% water, is equal to that of pure water, i.e., 320 J g^{-1} (Fig. 6A). At about 70–80 wt.% DPA, the enthalpy reaches a minimum (230 J g^{-1}), and it then increases to about 460 J g^{-1} at very high DPA concentration. When the enthalpy of melting of water is plotted per gram of sample (Fig. 6B), it decreases linearly with increasing DPA concentration and becomes zero at 100% DPA.

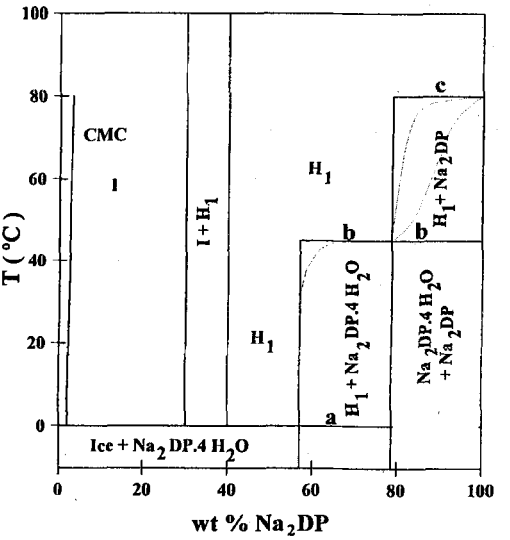

Fig. 5 Phase diagram for the Na_2DPA–water system: H: hexagonal phase; C: crystals; I: isotropic liquid

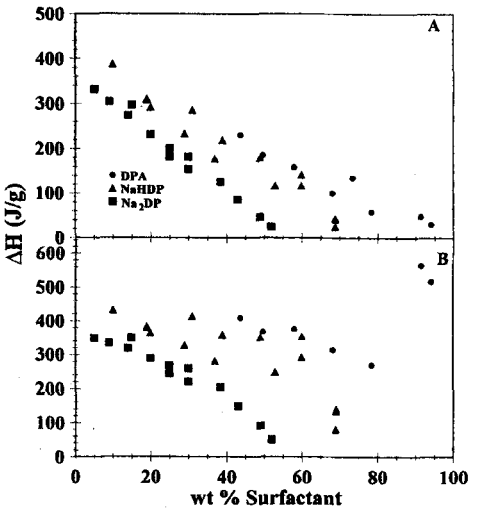

Fig. 6 Enthalpy of melting of water per gram of water (A) and per gram of sample (B) for the DPA–water (•); NaHDP–water (▲); and Na_2DP–water (■)

In the system NaHDP–water, the enthalpy of melting of water per gram of sample decreases linearly with increasing surfactant concentration, and it becomes zero at 73 wt.% NaHDP (Fig. 6A). At this concentration, there are about 5 molecules of water per molecule of surfactant. Extrapolation to 0 wt.% surfac-

tant yields values of $\Delta H_{melting}$ larger than those of pure water. $\Delta H_{melting}$ of water per gram of sample in the system Na_2DP–water decreases linearly with increasing surfactant concentration and it becomes zero at about 57 wt.% Na_2DP. At this concentration, there are about 11.2 molecules of water per molecule of surfactant. Again, extrapolation to zero surfactant concentration gives values abnormally high (352 J g^{-1}) for the enthalpy of melting of water.

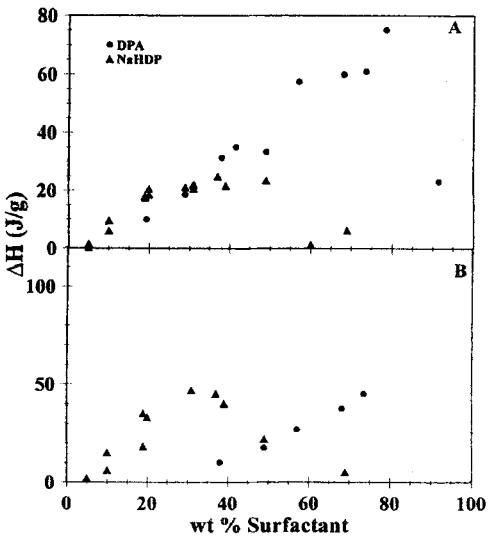

Fig. 7 (A) Enthalpy of transition **b** (crystalline solid+water→waxy solid) and (B) of transition **c** (waxy solid→mesophase) for the DPA–water (•) and the NaHDP–water system (▲)

Figure 7 reports the enthalpy of transitions **b** and **c** for the systems DPA–water and NaHDP–water. Transition **b** corresponds to the transformation of crystal into a 'waxy solid'. FTIR measurements on this phase indicate that the hydrocarbon network is 'liquid-like', but not completely disordered, whereas the hydrated, hydrogen-bonded polar network is still rigid [7]. ΔH for transformation **b** becomes zero at 16 wt.% for DPA and at 5.2 wt.% for NaHDP. Transformation **b** ends at point 1 in the phase diagram for DPA (Fig. 2), whereas in the system NaHDP–water the enthalpy of the transformation becomes zero at 71 wt.%, where the free water peak also disappears. Transformation **c**, in turn, corresponds to the phase transition between the 'waxy solid' and a lamellar phase. The enthalpies of transformations **b** and **c** increase linearly with increasing surfactant concentration for the system DPA–water, whereas they pass through a maximum at around 30–35 wt.% surfactant for the system NaHDP–water. In this concentration range, a phase transition finer timer texture lamellar (L_α) phase to a coarse texture lamellar (L_β) phase was detected (Fig. 4).

Discussion and conclusions

Even though the enthalpy of melting of water in the system DPA–water decreases linearly with increasing DPA concentration and becomes zero at 100% DPA (Fig. 6B), it is clear that some water is bound weakly to the surfactant molecule. The existence of bulk-like water and bound water can be deduced from the existence of two freezing peaks for water. One type of water behaves like free water and supercools at about −17°C. This peak loses intensity as the DPA concentration increases. The other peak appears at −20°C, with an average enthalpy of melting of 47.2±3.3 J g^{-1} of DPA. The constancy of this enthalpy when related to the mass of acid supports the hypothesis that this water is associated with the DPA headgroup. This appears to be true only when the systems is in a liquid phase, i.e. this association does not exist when the system is solid-like.

With NaHDP, about 5 molecules of water are strongly bound to the headgroup and the counterions. Inasmuch as the polar group in NaHDP is the same as in DPA, it is clear that much of this water is bound to Na^+. However, the presence of three peaks for the freezing of water suggests the presence of free water and of two types of interfacial water, one strongly bound to Na^+ and another more weakly bound to the polar groups, probably through hydrogen-bonding with the PO_3H^- headgroup. As expected, the amount of bound water in the system Na_2DP–water is around twice as much (11.2 molecules of water-molecule of surfactant) as in the system NaHDP–water, because the concentration of counterions is doubled. Hence, in the system Na_2DP–water, about 10 molecules of water are bound to Na^+ and 1 molecule of water is more weakly bound to the PO_3^{2-} headgroup through hydrogen-bonding.

Extrapolation of the plots of enthalpy of melting of water (Fig. 6) to zero surfactant concentration gives values larger than that for pure water for both NaHDP and Na_2DP. The entropy of melting at zero surfactant concentration for Na_2DP (24.3 J K^{-1} per mole of water) and for NaHDP (30.0 J K^{-1} per mole of water) are also larger than that for pure water (21.08 J K^{-1} per mole of water). Abnormally large values for enthalpy and entropy of melting have also been reported for this kind of system elsewhere [20, 21]. The entropy of melting decreases continuously with increasing surfactant concentration in the NaHDP and Na_2DP systems. These decreases suggest that there is an influence of the ions on the water molecules even at large dilution [22].

In the system DPA–water, complex phase behavior was observed (Fig. 2). Pure DPA exhibited the following sequence of phases with increasing temperature.

crystalline solid → waxy solid → cubic phase → isotropic liquid

whereas the DPA–water mixtures exhibited the following sequence of phases with increasing temperature:

crystalline solid + ice → crystalline solid + water → waxy solid → lamellar phase (L_α) → lamellar phase (L_β) → isotropic liquid

By contrast, the phase behavior of the systems of the sodium salts of DPA and water is quite different (Figs 4 and 5). For instance, in the system NaHDP–water only one hexagonal phase is detected at low surfactant concentrations, which changes into a lamellar phase as the surfactant concentration is increased, whereas in the system Na_2DP–water only a hexagonal phase is observed. The phase sequence with increasing temperature for the sodium surfactants in water is as follows:

crystalline solid + ice → crystalline solid + water → waxy solid → meso-phase → isotropic liquid

The enthalpies of two of these phase transitions were examined for the systems DPA–water and NaHDP–water: transition **b** (crystalline solid+water→waxy solid) and transition **c** (waxy solid→lamellar phase). For the system DPA–water, the enthalpies of both transitions increase with increasing DPA concentration (Fig. 7). These increases are related to the energy required to 'melt' the hydrocarbon chains of the crystalline structure to form the waxy solid, and to disrupt the polar association in the waxy solid to produce the lamellar phase. Both transitions shift to higher temperatures as the water content decreases because the presence of water disrupts the structures of the crystalline solid and the waxy solid. By contrast, the enthalpies of transitions **b** and **c** in the system NaHDP–water pass through a maximum at surfactant concentrations around 30–35 wt.% (Fig. 7). No explanation of this maximum is available as yet, but it is significant that, at the concentration where the maximum occurs, there is a transition from a fine texture lamellar phase (L_α) to a coarse texture (L_β) phase in this system (Fig. 4).

* * *

This work was supported by the Consejo Nacional de Ciencia y Tecnología de México (grant # 3319-E) and by the Consejo Nacional de Investigaciones Científicas y Técnicas de la República de Argentina.

References

1 A. A. Oswald, H. Huang, J. Huang and P. Valint, Jr., U. S. Patent, 4, 434, 062 (1984).
2 S. Kaneshina and M. Yamanaka, J. Colloid Interface Sci., 140 (1990) 474.
3 M. J. Blandamer, B. Briggs, J. Burgess, P. M. Cullis and G. Eaton, J. Chem. Soc. Faraday Trans., 87 (1991) 1169, 88 (1992) 2871.
4 H. Matsuki, R. Ichikawa, S. Kaneshina, H. Kamaya and I. Ueda, J. Colloid Interface Sci., 181 (1996) 362.
5 M. I. Kabachnik, Doblady Akad. Nauk. USSR, 3 (1956) 393.
6 G. Klose, A. G. Petrov, F. Volke, H. W. Meyer, G. Forster and W. Retting, Mol. Cryst. Liq. Cryst., 88 (1982) 109.
7 P. C. Schulz, M. Abrameto, J. E. Puig, J. F. A. Soltero-Martínez and A. González-Alvarez, Langmuir, 12 (1996) 3082.

8 M. Duprat, A. Shiri, Y,. Derbalis and N. Pebere in Electrochemical Methods in Corrosion Research, Materials Science Forum, M. Duprat (Ed.), Trans Tech.: Aedermannsdorf 1986. Vol. 8, p. 267.
9 O. Navrátil and P. Sládek, Collect. Czech. Chem. Commun., 59 (1994) 59.
10 K. J. Kuys and N. K. Roberts, Colloids Surf., 24 (1987) 1.
11 K. Czarniecki, A. Jaich, J. M. Janik, M. Rachwalsa, J. A. Janik, J. Krawczyk, K. Otnes, F. Volino and R. Ramasseul, J. Colloid Interface Sci., 92 (1983) 358.
12 A. Faure, J. Lovera, P. Grégoire and C. Chachaty, J. Chim. Phys., 82 (1985) 779.
13 N. Casillas, J. E. Puig, R. Olayo, T. J. Hart and E. I. Franses, Langmuir, 5 (1989) 384.
14 A. Goto, H. Yoshioka, H. Kishimoto and T. Fujita, Langmuir, 8 (1992) 441.
15 P. C. Schulz, J. E. Puig, G. Barreiro and L. A. Torres, Thermochim. Acta, 231 (1994) 239.
16 P. C. Schulz and A. L. M. Lelong, Rev. Latinoam. Quim., 7 (1967) 9.
17 A. L. M. Lelong and N. Miguens, Anales Asoc. Quim. Argentina, 62 (1974) 71.
18 D. Senatra and E. Zhou, Prog. Colloid Polym. Sci., 76 (1988) 106.
19 P. C. Schulz and A. L. M. Lelong, Anales Asoc. Quim. Argentina, 66 (1978) 11.
20 K. P. Antonsen and A. S. Hofmann in Poly(ethylene glycol) Chemistry, Biotechnical and Biomedical Applications, J. M. Harris (Ed.), Plenum Press, New York 1992, p . 15.
21 T. de Vringer, J. G. H. Joosten and H. E. Juninger, Colloid Polym. Sci., 264 (1986) 623.
22 N. Garti, A. Aserin, S. Ezrahi, I. Tiunova and G. Berkovic, J. Coll. Interf. Sci., 178 (1996) 60.